Inorganica Chimica Acta, *219* (1994) 179–186

Variation of the exchange interaction in oximato-bridged $Cu^{II}M^{II}$ dimers (M = Cu, Ni, Mn). Crystal structure of $[Cu(pdmg)Cu(bipy)(H_2O)_2](ClO_4)_2 \cdot H_2O$

Rafael Ruiz, Francesc Lloret and Miguel Julve*
Departament de Química Inorgànica, Facultat de Química, Universitat de València, Dr. Moliner 50, 46100 Burjassot (València) (Spain)

M. Carmen Muñoz
Departamento de Física Aplicada, Universidad Politécnica de València, Camino de Vera s/n, 46071 València (Spain)

Claudette Bois
Laboratoire de Chimie des Métaux de Transition, Université Pierre et Marie Curie, URA 419 CNRS, 75252 Paris (France)

(Received October 22, 1993; revised January 11, 1994)

Abstract

Three new dinuclear complexes of formula $[Cu(pdmg)Cu(bipy)(H_2O)_2](ClO_4)_2 \cdot H_2O$ (**1**), $[Cu(pdmg)Cu(terpy)](ClO_4)_2$ (**2**) and $[Cu(pdmg)Ni(cyclam)](ClO_4)_2 \cdot H_2O$ (**3**) (H_2pdmg = 3,3′-aminopropylenedinitrilobis(2-butanone-oxime); bipy = 2,2′-bipyridyl; terpy = 2,2′:6′,2″-terpyridyl; cyclam = 1,4,8,11-tetraazacyclotetradecane) have been synthesized. The structure of **1** has been determined by single-crystal X-ray diffraction. It crystallizes in the monoclinic system, space group $P2_1/a$, with $a = 14.160(3)$, $b = 21.300(2)$, $c = 10.208(2)$ Å, $\beta = 95.44(2)°$, $V = 3065(2)$ Å^3, $Z = 4$, $D_x = 1.68$ g cm^{-3}, μ(Mo Kα) = 16.3 cm^{-1}, $F(000) = 1584$ and $T = 291$ K. A total of 5263 reflections was measured over the range $1 \leq \theta \leq 25°$; of these, 2057 (independent and with $I \geq 2\sigma(I)$) were used in the structural analysis. The final R and R_w residuals were 0.062 and 0.064, respectively. The structure of **1** is made up of cationic $[Cu(pdmg)Cu(bipy)_2(H_2O)_2]^{2+}$ units, non-coordinated perchlorate anions and water of crystallization. The [Cu(pdmg)] fragment coordinates to the second copper(II) ion through its deprotonated oximate oxygens to afford a binuclear structure doubly bridged by the oximate groups in the *cis* arrangement. The $Cu(NO)_2Cu$ bridging network is bent, the dihedral angle being 151°. The intramolecular metal–metal distance is 3.691(2) Å. The magnetic behavior of **1**–**3** was investigated in the temperature range 50–300 K. The values of the exchange coupling constant J (the spin Hamiltonian being $\hat{H} = -J\hat{S}_A \cdot \hat{S}_B$) for **1**–**3** were −674, −174 and −204 cm^{-1}, respectively. The influence on the exchange coupling of the orientation of the magnetic orbitals and the number of unpaired electrons involved in the oximato-bridged $Cu^{II}M^{II}$ dimers (M = Cu, Ni, Mn) are analyzed and discussed.

Key words: Crystal structures; Copper complexes; Nickel complexes; Manganese complexes; Bidentate ligand complexes; Dinuclear complexes

Introduction

In a recent contribution, we investigated the dependence of the magnitude of the exchange interaction upon the nature of the bridging ligand (phenolato, oximato and oxamidato) in a series of dinuclear $Cu^{II}Mn^{II}$ complexes [1]. This study showed that the oxime group is one of the best bridging ligands to mediate strong antiferromagnetic coupling between paramagnetic centers $J(Cu^{II}Mn^{II}) = -50$ cm^{-1}) provided that a magnetic exchange pathway like that shown in Scheme 1 holds for each metal ion.

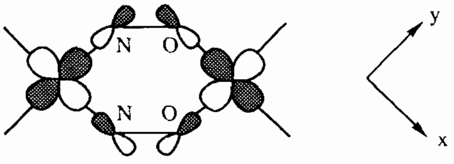

Scheme 1.

In the present work, we focus on the use of the mononuclear complex (3,3′-aminopropylenedinitrilobis(2-butanoneoximato)copper(II), hereafter noted Cu(pdmg) (Scheme 2), as a precursor of both homo- and hetero-polynuclear species [2] aiming at illustrating the influence on the magnitude of the exchange coupling

---

*Author to whom correspondence should be addressed.

SSDI 0020-1693(94)03825-9

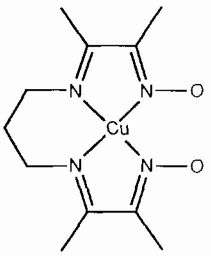

Scheme 2.

through the oximato bridge of (i) the relative orientation of the magnetic orbitals and (ii) the number of unpaired electrons of the metal centers. Along this line, we report here the preparation and magnetic characterization of three dinuclear complexes of formula [Cu(pdmg)Cu(bipy)$(H_2O)_2](ClO_4)_2 \cdot H_2O$ (**1**), [Cu(pdmg)Cu(terpy)]$(ClO_4)_2$ (**2**) and [Cu(pdmg)Ni(cyclam)]$(ClO_4)_2 \cdot H_2O$ (**3**) (H_2pdmg = 3,3′-aminopropylenedinitrilobis(2-butanoneoxime); bipy = 2,2′-bipyridyl; terpy = 2,2′:6′,2″-terpyridyl; cyclam = 1,4,8,11-tetraazacyclotetradecane) together with the crystal structure of the former.

Experimental

Reagents

All chemicals were of reagent grade quality and were purchased from commercial sources and used as received. The starting materials Cu(Hpdmg)$(ClO_4) \cdot H_2O$ and [Ni(cyclam)]$(ClO_4)_2$ were prepared by literature methods [3, 4]. Elemental analyses (C, H, N) were performed by the Microanalytical Service of the Universidad Autónoma de Madrid (Spain). Metal content was determined by atomic absorption spectrometry.

Caution: perchlorate salts of metal complexes with organic ligands are potentially explosive. We used only small amounts of material in the syntheses described herein (the preparations were carried out at the millimole scale). The resulting solutions were handled with care and evaporated slowly at room temperature.

Synthesis of the complexes

[Cu(pdmg)Cu(bipy)$(H_2O)_2](ClO_4)_2 \cdot H_2O$ (1)

Well-shaped dark red prismatic crystals of **1** which were suitable for X-ray analysis were obtained by slow evaporation of methanolic solutions of its dihydrate form which was prepared as previously reported [2]. They were filtered off, washed with cold methanol and diethyl ether, and stored over calcium chloride. *Anal.* Calc. for $C_{21}H_{32}Cl_2N_6O_{13}Cu_2$ (**1**): C, 32.57; H, 4.16; N, 10.85; Cu, 16.42. Found: C, 32.65; H, 4.00; N, 10.83; Cu, 16.03%.

[Cu(pdmg)Cu(terpy)]$(ClO_4)_2$ (2)

A mixture of $Cu(ClO_4)_2 \cdot 6H_2O$ (176 mg, 0.5 mmol) and terpy (117 mg, 0.5 mmol) dissolved in hot methanol (25 cm^3) was added to a warm absolute ethanolic solution (25 cm^3) containing Cu(Hpdmg)$(ClO_4) \cdot H_2O$ (210 mg, 0.5 mmol) and triethylamine (1 cm^3) under continuous stirring. Golden brown microcrystals of **2** deposited immediately. After cooling the solution to room temperature, the crystals were separated by filtration, washed with absolute ethanol and diethyl ether, and air-dried. *Anal.* Calc. for $C_{26}H_{29}Cl_2N_7O_{10}Cu_2$ (**2**): C, 39.16; H, 3.67; N, 12.29; Cu, 15.94. Found: C, 39.02; H, 3.71; N, 12.17; Cu, 15.65%.

[Cu(pdmg)Ni(cyclam)]$(ClO_4)_2 \cdot H_2O$ (3)

A warm acetonitrile solution (25 cm^3) of Ni(cyclam)$(ClO_4)_2$ (229 mg, 0.5 mmol) was added to a methanolic solution (25 cm^3) containing a mixture of Cu(Hpdmg)$(ClO_4) \cdot H_2O$ (210 mg, 0.5 mmol) and triethylamine (1 cm^3). The resulting solution was kept under gentle refluxing for 1 h. Small red–brown needles of **2** separated from this solution after a few days by slow evaporation in a hood at room temperature. They were filtered and recrystallized from methanol. *Anal.* Calc. for $C_{21}H_{44}Cl_2N_8O_{11}CuNi$ (**3**): C, 32.44; H, 5.66; N, 14.41; Cu, 8.17; Ni, 7.55. Found: C, 32.65; H, 5.69; N, 14.26; Cu, 7.98; Ni, 7.34%.

Magnetic measurements

Variable-temperature magnetic susceptibility measurements were carried out on crystalline samples in the range 50–300 K with a fully automatized AZTEC DSM8 pendulum-type susceptometer equipped with a TBT continuous-flow cryostat and a Brüker BE15 electromagnet, operating at 1.8 T. The apparatus was calibrated with $Hg[Co(NCS)_4]$. Corrections for the diamagnetism of **1**–**3** were estimated from Pascal's constants [5] as -348×10^{-6}, -337×10^{-6} and -370×10^{-6} cm^3 mol^{-1}, respectively. Magnetic susceptibility data were also corrected for temperature-independent paramagnetism and magnetization of the sample holder.

X-ray structure determination of 1

Diffraction data for a prismatic crystal of **1** of approximate dimensions 0.70×0.40×0.25 mm were collected at 291 K with Philips PW 1100 four-circle diffractometer. Cell data and details of the experimental conditions are given in Table 1. The unit-cell parameters were determined and refined from least-squares fitting of 25 carefully well centered reflections in the range $12 \leqslant \theta \leqslant 13°$. Two reference intensities which were recorded every 2 h throughout the data collection showed no sign of crystal deterioration. The θ range for data collection was 1–25°, the octants of data collected being $-16 \leqslant h \leqslant 16$, $0 \leqslant k \leqslant 25$ and $0 \leqslant l \leqslant 12$. Intensity data

TABLE 1. Crystal data and structure refinement for complex **1**

Molecular formula	$C_{21}H_{32}Cl_2CuN_6O_{13}$
Molecular weight	774.5
Crystal system	monoclinic
Space group	$P2_1/a$
a (Å)	14.160(3)
b (Å)	21.300(2)
c (Å)	10.208(2)
β (°)	95.44(2)
V (Å^3)	3065(2)
Z	4
D_{calc} (g cm^{-3})	1.68
Radiation	graphite monochromated Mo Kα (λ=0.71069 Å)
$F(000)$	1584
μ (cm^{-1})	16.3
Scan technique	ω–2θ
Scan speed (° min^{-1})	0.36–1.8
Scan width (°)	0.9+0.34 tan θ
No. measured reflections	2462
Cutoff observed data	$2.0\sigma(I)$
No. observed reflections	2057
No. reflections per parameter	5.2
R^a	0.062
$R_w{}^b$	0.064

$^aR=\Sigma(||F_o|-|F_c||)/\Sigma|F_o|$. $^bR_w=[\Sigma w(|F_o|-|F_c|)^2/\Sigma w|F_o|^2]^{1/2}$.

were corrected for Lorentz and polarization effects. An empirical absorption correction was also performed by using DIFABS [6].

The structure of **1** was solved by direct methods followed by successive Fourier synthesis and least-squares refinements carried out in four blocks (399 parameters). All non-hydrogen atoms were treated anisotropically. All hydrogen atoms could not be found on a ΔF map, and some of them were geometrically located; those concerning the crystallization water molecule were not introduced. All hydrogen atoms were given the same isotropic thermal parameter which was included in the final refinement. The function minimized was $\Sigma w(|F_o|-|F_c|)^2$ and each reflection was assigned a unit weight. Atomic scattering factors and corrections for anomalous dispersion were taken from ref. 7. The final R and R_w discrepancy indices were 0.062 and 0.064, respectively. The residual maximum and minimum peaks in the final difference synthesis were 0.46 and −0.54 e Å^{-3}. All crystallographic calculations were performed on a VAX 725 computer by means of the program CRYSTALS [7] and the molecular drawings were drawn with the CAMERON program [8]. Final atomic coordinates for non-hydrogen atoms and selected bond distances and angles are listed in Tables 2 and 3, respectively.

TABLE 2. Final atomic coordinates for non-hydrogen atoms^a and equivalent isotropic thermal parameters for complex **1**

Atom^b	x/a	y/b	z/c	$U_{eq}{}^c$ (Å^2)
Cu(1)	0.2619(1)	0.51499(9)	0.1346(1)	0.0460
Cu(2)	0.0711(1)	0.51824(9)	−0.1380(2)	0.0500
N(1)	0.3190(8)	0.4441(6)	0.243(1)	0.0494
N(2)	0.3357(9)	0.5822(6)	0.230(1)	0.0592
N(3)	0.1957(8)	0.5883(5)	0.050(1)	0.0443
N(4)	0.1730(8)	0.4478(5)	0.071(1)	0.0440
N(5)	−0.0145(8)	0.4579(6)	−0.247(1)	0.0488
N(6)	0.0137(9)	0.5783(7)	−0.276(1)	0.0476
O(1)	0.1259(8)	0.5897(5)	−0.0408(9)	0.0598
O(2)	0.0957(7)	0.4515(4)	−0.0103(8)	0.0492
O(3)	0.3634(7)	0.5019(5)	−0.0238(9)	0.0707
O(4)	0.2042(7)	0.4979(5)	−0.2516(9)	0.0730
C(1)	0.401(1)	0.4491(9)	0.338(2)	0.0686
C(2)	0.459(1)	0.507(1)	0.310(2)	0.0872
C(3)	0.413(1)	0.5719(8)	0.331(2)	0.0587
C(4)	0.312(1)	0.6374(8)	0.190(2)	0.0567
C(5)	0.234(1)	0.6424(7)	0.091(1)	0.0470
C(6)	0.278(1)	0.3918(8)	0.213(2)	0.0563
C(7)	0.196(1)	0.3922(6)	0.122(1)	0.0431
C(8)	−0.018(1)	0.3960(8)	−0.228(2)	0.0650
C(9)	−0.082(1)	0.3595(8)	−0.317(2)	0.0669
C(10)	−0.138(1)	0.386(1)	−0.406(2)	0.0816
C(11)	−0.133(1)	0.450(1)	−0.427(2)	0.0678
C(12)	−0.070(1)	0.4865(9)	−0.346(1)	0.0482
C(13)	−0.058(1)	0.5539(7)	−0.362(1)	0.0419
C(14)	−0.108(1)	0.591(1)	−0.452(2)	0.0631
C(15)	−0.086(1)	0.653(1)	−0.457(2)	0.0729
C(16)	−0.016(2)	0.6786(8)	−0.380(2)	0.0804
C(17)	0.036(1)	0.6382(9)	−0.286(2)	0.0655
C(41)	0.361(1)	0.6977(8)	0.248(2)	0.0812
C(51)	0.189(1)	0.7020(7)	0.031(2)	0.0651
C(61)	0.316(1)	0.3296(9)	0.277(2)	0.0898
C(71)	0.138(1)	0.3359(7)	0.075(2)	0.0559
Cl(1)	0.3264(4)	0.3437(3)	−0.2908(6)	0.0861
Cl(2)	0.6465(4)	0.3461(3)	0.2917(6)	0.0801
O(5)	0.248(1)	0.3534(7)	−0.227(2)	0.1200
O(6)	0.404(1)	0.3240(9)	−0.214(2)	0.1688
O(7)	0.308(2)	0.291(1)	−0.374(2)	0.1857
O(8)	0.344(1)	0.3958(8)	−0.365(2)	0.1349
O(9)	0.592(2)	0.322(1)	0.189(3)	0.2160
O(10)	0.729(1)	0.318(1)	0.293(2)	0.1779
O(11)	0.653(1)	0.4075(8)	0.306(2)	0.1674
O(12)	0.602(2)	0.328(1)	0.393(3)	0.2144
O(13)	0.520(2)	0.6062(9)	−0.005(2)	0.1757

^{a}e.s.d.s given in parentheses. ^{b}Atoms Cl(1), O(5), O(6), O(7), O(8) and Cl(2), O(9), O(10), O(11), O(12) refer to the two perchlorate anions while O(13) is the oxygen from the water molecule. $^cU_{eq}=(1/3)\Sigma_i\Sigma_j U_{ij}a_i^* a_j^* \mathbf{a}_i\mathbf{a}_j$.

Results and discussion

Description of the structure of 1

The structure of complex **1** consists of dinuclear $[Cu(pdmg)Cu(bipy)(H_2O)_2]^{2+}$ cations, uncoordinated perchlorate anions and crystallization water molecules. The [Cu(pdmg)] fragment coordinates to the second copper(II) ion through the deprotonated oximate ox-

TABLE 3. Selected bond distances (Å) and angles (°) for complex **1**

Cu(1)–N(1)	2.00(1)	Cu(2)–N(5)	2.02(1)
Cu(1)–N(2)	1.97(1)	Cu(2)–N(6)	2.02(1)
Cu(1)–N(3)	1.98(1)	Cu(2)–O(1)	1.94(1)
Cu(1)–N(4)	1.97(1)	Cu(2)–O(2)	1.938(9)
Cu(1)–O(3)	2.280(9)	Cu(2)–O(4)	2.345(9)
N(1)–Cu(1)–N(2)	96.2(5)	N(2)–Cu(2)–N(6)	80.7(5)
N(1)–Cu(1)–N(3)	171.5(5)	N(5)–Cu(2)–O(1)	165.7(5)
N(1)–Cu(1)–N(4)	81.1(5)	N(5)–Cu(2)–O(2)	87.9(5)
N(1)–Cu(1)–O(3)	93.0(4)	N(5)–Cu(2)–O(4)	94.5(4)
N(2)–Cu(1)–N(3)	81.3(5)	N(6)–Cu(2)–O(1)	88.5(5)
N(2)–Cu(1)–N(4)	168.2(5)	N(6)–Cu(2)–O(2)	166.0(5)
N(2)–Cu(1)–O(3)	95.6(4)	N(6)–Cu(2)–O(4)	93.5(4)
N(3)–Cu(1)–N(4)	99.7(5)	O(1)–Cu(2)–O(2)	101.2(4)
N(3)–Cu(1)–O(3)	95.1(4)	O(1)–Cu(2)–O(4)	95.5(4)
N(4)–Cu(1)–O(3)	96.0(4)	O(2)–Cu(2)–O(4)	95.5(4)
Cu(1)–N(3)–O(1)	129.2(10)	Cu(2)–O(1)–N(3)	126.3(9)
Cu(1)–N(4)–O(2)	129.1(9)	Cu(2)–O(2)–N(4)	123.8(8)

ygens to afford a dinuclear entity doubly bridged by oximate groups in the *cis* arrangement. A perspective drawing of the dinuclear unit with the atom numbering scheme is depicted in Fig. 1.

The coordination geometry around both copper atoms is distorted square pyramidal. The four nitrogen atoms of the pdmg ligand at Cu(1) and two oximate oxygen atoms and the two bipyridyl nitrogen atoms at Cu(2) build the corresponding basal planes; the fifth coordination position of the square pyramids about the metal ions is occupied by weakly bound water molecules (2.280(9) and 2.345(9) Å for Cu(1)–O(3) and Cu(2)–O(4), respectively). The four nitrogen atoms from the pdmg group are practically coplanar (the maximum deviation of these four atoms from their least-squares plane is 0.04 Å at N(1)) whereas the Cu(1) atom is slightly displaced from this mean plane by 0.170 Å towards the axial water oxygen O(3). The four Cu(1)–N bond lengths lie in the range 1.97(1)–2.00(1) Å. These values are slightly elongated when compared with the Cu–N bonds of the related [Cu(pdmg)Cu(phen)-$(CH_3OH)_2](ClO_4)_2$ complex [2] although they are common for in-plane Cu–N (oxime) distances [9–15]. The bond angles around Cu(1) from the six-membered rings (96.2(5) and 99.7(5)° for N(1)–Cu(1)–N(2) and N(3)–Cu(1)–N(4), respectively) are systematically greater than those from the five-membered chelate ones (81.1(5) and 81.3(5)° for N(1)–Cu(1)–N(4) and N(2)–Cu(1)–N(3), respectively) as observed in the structures of the complexes [Cu(pdmg)Cu(phen)-$(CH_3OH)_2](ClO_4)_2$ [2], Cu(Hpdmg)$ClO_4\cdot\frac{1}{2}CH_3OH$ [10], $[Cu(Hpdmg)]_2(ClO_4)_2$ [11] and $[Cu\{Cu(pdmg)\}_2](ClO_4)_2$ [13]. It should be noted that the two compounds that contain Hpdmg$^-$ as a ligand are polymeric. Both structures have in common the coordination of the diazadioxime as a tetradentate ligand toward copper(II). However, the presence of an oxime oxygen atom of other Cu(Hpdmg) units in the axial position of the metal ion leads to a dimeric structure in the case of the methanol solvate and to zigzag chains in $[Cu(Hpdmg)]_2(ClO_4)_2$. Dealing with Cu(2), the Cu–N(bipy) bond lengths (2.02(1) Å for both Cu(2)–N(5) and Cu(2)–N(6)) are larger than that of Cu–O(oxime) (1.94(1) and 1.938(9) Å for Cu(2)–O(1) and Cu(2)–O(2), respectively) in agreement with previous data of the related dinuclear [Cu(pdmg)Cu(phen)$(CH_3OH)_2](ClO_4)_2$ [2] and trinuclear $[Cu_3(dmg)(bipy)_2(CH_3OH)_2(NO_3)_2]$ and $[Cu_3(dpg)(bipy)_2(CH_3OH)_2(NO_3)_2]$ [12] (dmg^{2-} and dpg^{2-} are the dianions of dimethylglyoxime and diphenylglyoxime, respectively). The Cu(2) atom sticks out of its mean basal plane by 0.166 Å in the direction of the axially-bound water molecule. The angle sub-

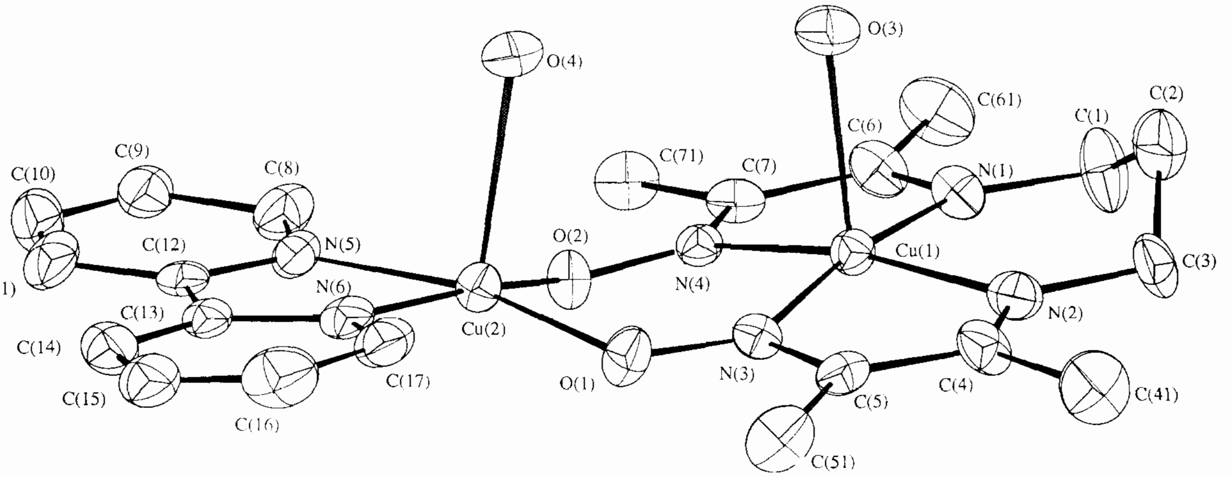

Fig. 1. Perspective view of the cationic unit of complex **1** with the numbering scheme. Thermal ellipsoids are drawn at the 30% probability level. Hydrogen atoms were omitted for clarity.

tended at Cu(2) by bipy (80.7(5)° for N(5)–Cu(2)–N(6)) is significantly smaller than 90° as expected due to the geometric constraints of a bipyridyl ring system. The dihedral angle between the mean basal planes around the copper atoms is 162.6°. The central six-membered Cu(1)N(3)O(1)Cu(2)O(2)N(4) ring exhibits a boat conformation, the Cu(1) and Cu(2) atoms being 0.185 and 0.277 Å above the mean plane towards the axially coordinated water molecules.

The pdmg group acts simultaneously as a tetradentate (Cu(1)) and as a bidentate (Cu(2)) ligand through its nitrogen and oxygen atoms, respectively, leading to the formation of alternating five- and six-membered chelating rings around Cu(1). Each five-membered ring is quite planar (the largest deviation is 0.04 Å at N(1) for the Cu(1)N(1)C(6)C(7)N(4) ring). The four $C(sp^2)$–$C(sp^3)$ bond lengths average 1.53 Å as expected for a carbon–carbon single bond distance. A significant reduced value is observed for the average value of the two $C(sp^2)$–$C(sp^2)$ bond distances (1.43 Å) because of the smaller single-bond radius for carbon in trigonal hybridization. As far as the carbon–nitrogen bonds are concerned, the shortening of the imine and oxime bonds (average value 1.30 Å) with respect to the remaining ones (average value 1.45 Å for C(1)–N(1) and C(3)–N(2) bonds) reflects the partial double character in the former versus the single one in the latter. Bipy coordinates to Cu(2) in a chelating fashion. The pyridyl rings are planar as expected, but the ligand as a whole is not planar (the dihedral angle between the pyridyl rings is 6.1°). Average values of the C–C and C–N bond lengths (1.37(2) and 1.35(2) Å, respectively) are in agreement with that reported for free 2,2′-bipyridyl [16].

The values of the $O(3)\cdots O(13^{ii})$, $O(4)\cdots O(11^{ii})$, $O(6)\cdots O(13^{ii})$ and $O(9)\cdots O(13^{ii})$ ((ii) = $1-x$, $1-y$, $-z$) distances (2.83(2), 2.95(2), 2.82(3) and 2.79(3) Å, respectively) suggest the occurrence of hydrogen bonding involving one perchlorate anion, the two coordinated water molecules and the lattice water. The *cis* arrangement of O(3) and O(4) with respect to the mean planes of the dinuclear unit is thus stabilized by hydrogen bonding (see Fig. 2). The intramolecular $Cu(1)\cdots Cu(2)$ separation is 3.691(2) Å, a value which is significantly shorter than that reported for the trinuclear $[Cu(dioxim)(CuL)_2]^{2+}$ complexes [12]. The bent structure in **1** versus the coplanar trinuclear skeleton in $[Cu(dioxim)(CuL)_2]^{2+}$ species accounts for this shortening. The intradimer metal–metal separation is practically identical to the shortest intermolecular metal–metal distance (3.697(2) Å for $Cu(2)\cdots Cu(2^i)$ with (i) = $-x$, $1-y$, $-z$). This is due to the fact that Cu(2) completes a very distorted octahedral environment through a very weak interaction with $O(2^i)$ (2.99(1) Å for Cu(2)–$O(2^i)$) and steric effects or electrostatic repulsion between Cu(2) and $Cu(2^i)$ causes a significant bending of the $Cu(NO)_2Cu$ core (the dihedral angle between the planes Cu(1)N(3)N(4)O(1)O(2) and Cu(2)O(1)O(2) is 151°).

Magnetic properties

The magnetic properties of **1** and **2** are compared in Fig. 3 in the form of χ_M versus T plot χ_M being the molar magnetic susceptibility and T the temperature. They are characteristic of antiferromagnetically coupled copper(II) pairs with a rounded maximum above the room temperature for **1** and centered at *c*. 150 K for **2**. Consequently, the magnetic data of **1** and **2** were

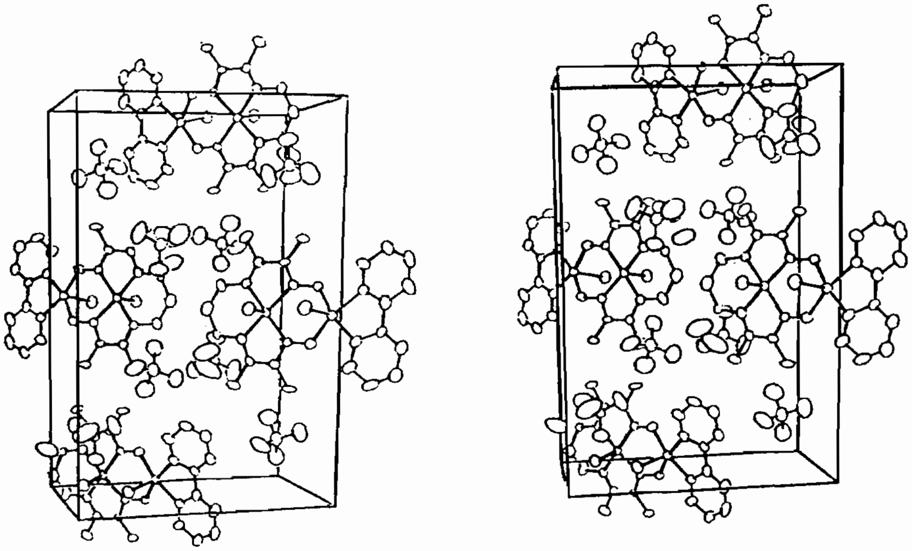

Fig. 2. A stereoscopic drawing of **1** down the *c* axis (the *b* axis is vertical).

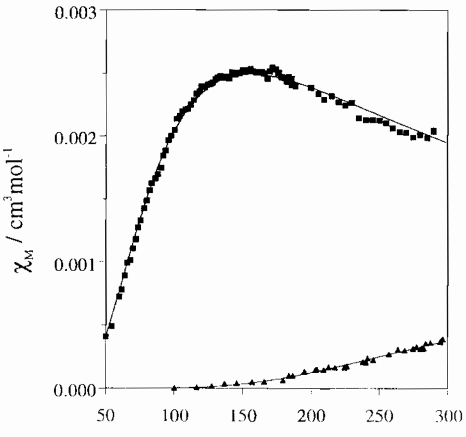

Fig. 3. Thermal dependence of χ_M for **1** (▲) and **2** (■). The solid lines correspond to the best theoretical fits.

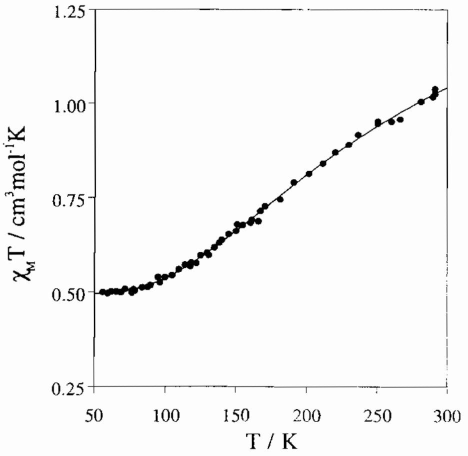

Fig. 4. Thermal dependence of $\chi_M T$ for **3**: ●, experimental data; —, best theoretical fit.

treated with a simple Bleaney–Bowers expression (eqn. (1))

$$\chi_M = (2N\beta^2 g^2/kT)[3 + \exp(-J/kT)] \qquad (1)$$

where the symbols N, β, g and k have their usual meanings and J is the singlet–triplet energy gap. Least-squares fitting of the experimental data through eqn. (1) by minimizing the reliability factor $R(R = \Sigma[(\chi_M T)^{obs} - (\chi_M T)^{calc}]^2/\Sigma[(\chi_M T)^{obs}]^2)$ leads to $J = -674$ cm^{-1} and $g = 2.06$ ($R = 6.9 \times 10^{-4}$) for **1** and to $J = -174$ cm^{-1} and $g = 2.08$ ($R = 2.3 \times 10^{-4}$) for **2**.

The magnetic behavior of **3** is shown in Fig. 4 in the form of a $\chi_M T$ versus T plot. At room temperature, $\chi_M T$ is equal to 1.03 cm^3 mol^{-1} K, a value which is significantly reduced with respect to what is expected for magnetically non-interacting copper(II) and nickel(II) ions. When the temperature is lowered, $\chi_M T$ continuously decreases and finally reaches a plateau around 80 K with $\chi_M T = 0.49$ cm^3 mol^{-1} K. $\chi_M T$ is then constant down to 50 K. This behavior closely follows what is expected for an isolated and antiferromagnetically coupled Cu(II)Ni(II) pair, with local spins $S_{Cu} = 1/2$ and $S_{Ni} = 1$. The antiferromagnetic interaction within the pair gives rise to a ground doublet state and an excited quartet state separated by $-3J/2$. The plateau below 80 K corresponds to the temperature range where only the ground doublet state is thermally populated. Consequently, the magnetic data were interpreted with the theoretical law appropriate for an isolated Cu(II)Ni(II) pair (eqn. (2)),

$$\chi_M T = (N\beta^2/4k)[g_{1/2}{}^2 + 10g_{3/2}{}^2 \times \exp(3J/2kT)]/[1 + 2\exp(3J/2kT)] \qquad (2)$$

where J is the interaction parameter occurring in the spin Hamiltonian $-JS_{Cu} \cdot S_{Ni}$, and $g_{1/2}$ and $g_{3/2}$ are the Zeeman factors associated with the doublet and quartet spin states, respectively. The least-squares fitting of the experimental data through eqn. (2) leads to $J = -204$ cm^{-1}, $g_{1/2} = 2.30$ and $g_{3/2} = 2.18$ ($R = 1.0 \times 10^{-4}$). The values of $g_{1/2}$ and $g_{3/2}$ may be related to the local Zeeman factors g_{Ni} and g_{Cu}, assumed to be isotropic, through eqn. (3) [17, 18]. The values of g_{Ni} and g_{Cu} deduced from eqn. (3) are found to be equal to 2.24 and 2.06, respectively.

$$g_{1/2} = (4g_{Ni} - g_{Cu})/3; \quad g_{3/2} = (2g_{Ni} + g_{Cu})/3 \qquad (3)$$

The J values for **1**–**3** and that of the related oximato-bridged compounds of formula [Cu(pdmg)Mn(phen)$_2$](ClO$_4$)$_2$·2.5H$_2$O (**4**) [1], [Cu(pdmg)Cr(salen)]ClO$_4$ (**5**) [19] and [Cu(dmg)$_2$Mn(CH$_3$COO)]·2H$_2$O (**6**) [20] (phen = 1,10-phenanthroline; salen^{2-} = N,N'-ethylenebis(salicylideneiminate) are listed in Table 4. In the light of these values, two points deserve to be discussed: (i) the different magnitude of J in the Cu^{II}Cu^{II} compounds; (ii) the decrease of the antiferromagnetic coupling when going from Cu^{II}Cu^{II} to Cu^{II}Mn^{II} species.

Dealing with the first point, values of $-J$ up to 850 cm^{-1} have been reported for oximato-bridged dinuclear copper(II) complexes in which the double oximate adopts the *cis* conformation with a terminal bidentate ligand as in **1** [2, 15]. In these cases, we are dealing with $d_{x^2-y^2}$ type magnetic orbitals which are centered on each copper(II) ion and partially delocalized through the oximato bridge (see Scheme 1). The strong anti-

TABLE 4. Exchange parameters for oximato-bridged complexes

Compound	J (cm^{-1})	$n_A n_B J$ (cm^{-1})	Reference
Cu^{II}Cu^{II} (**1**)	−674	−674	this work
Cu^{II}Cu^{II} (**2**)	−174		this work
Cu^{II}Ni^{II} (**3**)	−204	−408	this work
Cu^{II}Mn^{II} (**4**)	−50	−250	1
Cu^{II}Cr^{III} (**5**)	25	75	19
Cu^{II}Mn^{III} (**6**)	52	208	20

ferromagnetic coupling observed is due to the large σ in-plane overlap between the coplanar $d_{x^2-y^2}$ magnetic orbitals. Structural distortions in **1** such as its bent structure (the dihedral angle in the $Cu(NO)_2Cu$ core is 29°) and the deviations of copper atoms from the mean basal planes (*c.* 0.17 Å) would account for the somewhat reduced value of the antiferromagnetic coupling for this compound in this family. As far as complex **2** is concerned, the presence of terpy as a tridentate terminal ligand causes a very strong decrease of the intramolecular antiferromagnetic coupling. It is well known that tridentate N-donors such as terpy coordinate to copper(II) occupying three of the four short equatorial positions. Consequently, the bidentate Cu(pdmg) ligand can coordinate to $Cu(terpy)^{2+}$ through its two oxime-oxygen atoms, one filling the remaining equatorial position and the other one occupying an axial position (see Scheme 3).

In this situation, only one of the two oximato bridges is able to mediate significant exchange coupling. Let us analyze it by using the model of interaction of localized non-orthogonal magnetic orbitals proposed by Kahn and Briat [21]. In this context, the J value for a dinuclear unit is given by eqn. (4) [22]

$$J = 2j + 4\beta S \qquad (4)$$

where S is the overlap integral between the two magnetic orbitals centered on each copper(II) ion and β and j are their monoelectronic resonance (<0) and bielectronic exchange integrals, respectively. When j is sufficiently weak to be negligible with respect to βS we have (eqn. (5))

$$|J| \sim 4\beta S \sim S^2 \qquad (5)$$

The larger the value of S, the greater the antiferromagnetic coupling. In the case of complex **1** (Scheme 1), the two $d_{x^2-y^2}$ magnetic orbitals overlap through both N–O bridges. However, for complex **2**, the overlapping occurs only through one of the two N–O bridges due to the orbital reversal [23] caused by the presence of terpy as terminal ligand. Consequently, given that the ratio between overlap integrals of **1** and **2** is $S_2/S_1 = 1/2$, the J value for **2** is predicted to be one fourth of that for **1**. In fact, the value of $-J$ for **2** agrees quite well with this prediction ($674/4 \approx 168$ versus 174 cm^{-1}).

Finally, as far as the second point is concerned, when one of the metal ions has more than one unpaired electron (i.e. nickel(II) or manganese(II)) the experimental J parameter must be decomposed into a sum of individual contributions, $J_{\mu\nu}$, involving each pair of magnetic orbitals implicated in the exchange phenomenum (eqn. (6)) [24]

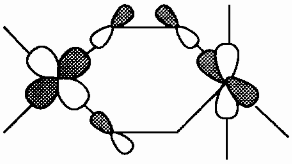

Scheme 3.

$$J = (1/n_A n_B) \sum_{\mu=1}^{n_A} \sum_{\nu=1}^{n_B} J_{\mu\nu} \qquad (6)$$

where n_A and n_B are the number of unpaired electrons associated with the transition metal ions A and B, respectively. Equation (6) shows how the magnitude of the net antiferromagnetic interaction is not properly described by J but by $n_A n_B J$, which has also been included in Table 4. At this stage, it seems easy to identify the mean factors causing the decrease of the product $n_A n_B/J/$ when n_B increases from 1 to 5, n_A being equal to 1, in this series. The first one is the increasing number of ferromagnetic terms $J_{\mu\nu}$ in eqn. (6) involving pairs of orthogonal magnetic orbitals (i.e. with $S=0$ in eqn. (4)) for the added unpaired electrons. It is well established that the more extended the bridge, the weaker the ferromagnetic coupling [25]. The present case deals with a diatomic bridging entity and important ferromagnetic contributions can be predicted. In fact, important ferromagnetic interactions occur in the $Cu^{II}Cr^{III}$ and $Cu^{II}Mn^{III}$ compounds (**5** and **6** in Table 4) due to the strict orthogonality between the magnetic orbitals which are involved. From the expressions of J for **5** and **6** (eqns. (7) and (8)) a rough value of

$$J(Cu^{II}Cr^{III}) = 1/3(J_{x^2-y^2,xy} + J_{x^2-y^2,xz} + J_{x^2-y^2,yz}) = 25\ cm^{-1} \qquad (7)$$

$$J(Cu^{II}Mn^{III}) = 1/4(J_{x^2-y^2,xy} + J_{x^2-y^2,xz} + J_{x^2-y^2,yz} + J_{x^2-y^2,z^2}) = 52\ cm^{-1} \qquad (8)$$

c. 130 cm^{-1} could be expected for the ferromagnetic term $J_{x^2-y^2,z^2}$.

The second factor to be considered is the magnitude of the antiferromagnetic term $J_{x^2-y^2,x^2-y^2}$. Values of *c.* -540 and -460 cm^{-1} for this term in compounds **3** and **4**, respectively, can be easily inferred through eqns. (9) and (10) by introducing the values of the above

$$J(Cu^{II}Ni^{II}) = 1/2(J_{x^2-y^2,x^2-y^2} + J_{x^2-y^2,z^2}) = -204\ cm^{-1} \qquad (9)$$

$$J(Cu^{II}Mn^{II}) = 1/5(J_{x^2-y^2,x^2-y^2} + J_{x^2-y^2,xy} + J_{x^2-y^2,xz} + J_{x^2-y^2,yz} + J_{x^2-y^2,z^2}) = -50\ cm^{-1} \qquad (10)$$

mentioned ferromagnetic terms in them. Keeping in mind that the value of this term is -674 cm^{-1} for **1**, one finds that the magnitude of $-J_{x^2-y^2,x^2-y^2}$ in the family $Cu^{II}B^{II}$ (B = Cu, Ni, Mn) follows the trend Cu > Ni > Mn. Two factors would account for this reduction: the lengthening of the metal to oxime-oxygen bond distances and the increase of the energy of the d orbitals when going from Cu(II) to Ni(II) and Mn(II). The combination of these two factors leads to a progressive decrease of spin density delocalization on the bridge when going from Cu(II) to Mn(II) and, consequently, to a decrease of the exchange interaction through the $d_{x^2-y^2}$ exchange pathway as observed.

Supplementary material

Tables of thermal parameters, non-essential bond distances and angles, least-squares planes (7 pages) as well as a listing of observed and calculated structure factors (7 pages) are available from the authors on request.

Acknowledgements

Financial support from the Comisión Interministerial de Ciencia y Tecnología (Project PB91-0807-C02-01) and the Programa de Acciones Integradas Hispano-Francesas are gratefully acknowledged. R.R. acknowledges the Conselleria de Cultura, Educació i Ciència de la Generalitat Valenciana for a doctoral grant.

References

1 R. Ruiz, F. Lloret, M. Julve, J. Faus, M.C. Muñoz and X. Solans, *Inorg. Chim. Acta, 213* (1993) 261.

2 D. Luneau, H. Oshio, H. Okawa, M. Koikawa and S. Kida, *Bull. Chem. Soc. Jpn., 63* (1990) 2212.

3 R.R. Gagné, *J. Am. Chem. Soc., 98* (1976) 6709.

4 B. Bosnich, M.L. Tobe and G.A. Webb, *Inorg. Chem., 4* (1965) 1109.

5 A. Earshaw, *Introduction to Magnetochemistry,* Academic Press, London, 1968.

6 N. Walker and D. Stuart, *Acta Crystallogr., Sect. A, 39* (1983) 156.

7 J.R. Carruthers and D.W.J. Watkins, *CRYSTALS,* an advanced crystallographic computer program, Chemical Crystallography Laboratory, University of Oxford, UK, 1985.

8 L.J. Pearce and D.J. Watkins, *CAMERON Program,* Chemical Crystallography Laboratory, University of Oxford, UK, 1992.

9 A. Vaciago and L. Zambonelli, *J. Chem. Soc. A,* (1970) 218.

10 J.A. Bertrand, J.N. Smith and D.G. Van Derveer, *Inorg. Chem., 16* (1977) 1484.

11 Y.M. Wang, C.C. Wang, S.L. Wang and C.S. Chung, *Acta Crystallogr., Sect. C, 46* (1990) 1770.

12 H. Okawa, M. Koikawa, S. Kida, D. Luneau and H. Oshio, *J. Chem. Soc., Dalton Trans.,* (1990) 469.

13 D. Luneau, H. Oshio, H. Okawa and S. Kida, *J. Chem. Soc., Dalton Trans.,* (1990) 2283.

14 P. Chaudhuri, M. Winter, B.P.C. Della Védova, E. Bill, A. Trautwein, S. Gehring, P. Fleischauer, B. Nuber and J. Weiss, *Inorg. Chem., 30* (1991) 2148.

15 R. Ruiz, J. Sanz, B. Cervera, F. Lloret, M. Julve, C. Bois, J. Faus and M.C. Muñoz, *J. Chem. Soc., Dalton Trans.,* (1993) 1623.

16 L.L. Mervit and E.D. Schroeder, *Acta Crystallogr., 9* (1956) 801.

17 R.P. Scaringe, D. Hodgson and W.E. Hatfield, *Mol. Phys., 35* (1978) 701.

18 D. Gatteschi and A. Bencini, in R.D. Willet, D. Gatteschi and O. Kahn (eds.), *Magneto-Structural Correlations in Exchange Coupled Systems,* NATO ASI Ser. C, Vol. 140, Reidel, Dordrecht, Netherlands, 1984.

19 Z.J. Zhong, H. Okawa, N. Matsumoto, H. Sakiyama and S. Kyda, *J. Chem. Soc., Dalton Trans.,* (1991) 497.

20 F. Lloret, R. Ruiz, M. Julve, J. Faus, Y. Journaux, I. Castro and M. Verdaguer, *Chem. Mater., 4* (1992) 1150.

21 O. Kahn and B. Briat, *J. Chem. Soc., Faraday Trans., 72* (1976) 268.

22 (a) J.J. Girerd, M.F. Charlot and O. Kahn, *Mol. Phys., 34* (1977) 1063; (b) O. Kahn and M.F. Charlot, *Nouv. J. Chim., 4* (1980) 567.

23 (a) J.J. Girerd, O. Kahn and M. Verdaguer, *Inorg. Chem., 19* (1980) 274; (b) M. Julve, M. Verdaguer, O. Kahn, A. Gleizes and M. Philoche-Levisalles, *Inorg. Chem., 23* (1984) 3808; (c) Y. Journaux, J. Sletten and O. Kahn, *Inorg. Chem., 24* (1985) 4063; (d) G. De Munno, M. Julve, M. Verdaguer and G. Bruno, *Inorg. Chem., 32* (1993) 2215; (e) R. Costa, A. García, J. Ribas, T. Mallah, Y. Journaux, J. Sletten, X. Solans and V. Rodríguez, *Inorg. Chem., 32* (1993) 3733.

24 (a) O. Kahn, *Struct. Bonding (Berlin), 68* (1987) 89; (b) O. Kahn, P. Tola and H. Coudanne, *Chem. Phys., 42* (1979) 355; (b) P. Tola, O. Kahn, C. Chauvel and H. Coudanne, *Nouv. J. Chim., 1* (1979) 467; (c) S.L. Lambert, L.S. Clifford, R.R. Gagné and D.N. Hendrickson, *Inorg. Chem., 21* (1982) 68.

25 O. Kahn, *Comments Inorg. Chem., 3* (1984) 105.